Journal of Nuclear Materials 572 (2022) 154027

Contents lists available at ScienceDirect

Journal of Nuclear Materials

journal homepage: www.elsevier.com/locate/jnucmat

Very high burnup spent fuel corrosion & leaching under hydrogen conditions

A. Puranen[a,*], L-Z. Evins[a,b], A. Barreiro[a,c], O. Roth[a,b], K. Spahiu[a,b]

[a] AB SVAFO, Uranvägen, 611 23, Nyköping, Sweden
[b] Swedish Nuclear Fuel and Waste Management Co, Sweden
[c] Studsvik Nuclear AB, Nyköping, Sweden

ARTICLE INFO

Article history:
Received 23 March 2022
Revised 6 September 2022
Accepted 8 September 2022
Available online 13 September 2022

Keywords:
Spent fuel
Nuclear Fuel
UO_2
Dissolution
Hydrogen

ABSTRACT

This paper concerns a very high burnup UO_2 spent nuclear fuel leaching experiment performed under high hydrogen pressure conditions (5 MPa H_2 initially) in simplified granitic groundwater. Following an initial release after start-up the results demonstrate that the concentrations of redox sensitive elements such as Tc, U, Np and Pu stabilize at the solubility limits of their reduced oxide forms. The release of non-redox sensitive elements such as Cs also ceased within a year. Together these observations indicate that the hydrogen overpressure resulted in reducing conditions that suppresses fuel matrix corrosion. Following an initially rather rapid release of fission gases Kr and Xe, the release also ceases towards the end of the experiment, although at a surprisingly high released fraction of the inventory. In this experiment the fuel was cut from the rod, crushed in a vice and pre-leached under semi aerated conditions for 9 days before transitioning to conditions of high hydrogen overpressure and the resulting apparent inhibition of further corrosion or dissolution of the fuel matrix. These results are in contrast to our previous experiments with other portions of fuel from the same rod under similar hydrogen conditions, but with extensive dry milling and fuel corrosion in aerated conditions, prior to the transitions to hydrogen conditions. The results thus tentatively support the conclusion that preceding oxidation of the fuel surfaces may limit the potential for hydrogen to suppress fuel corrosion and dissolution.

1. Introduction

Plans for deep geological disposal of spent nuclear fuel may involve burial of canisters approximately 500 m underground, where conditions are expected to be anoxic. The disposal concepts often involve canisters with a significant iron component, such as the iron insert in the Swedish KBS-3 design [1,2]. These canisters constitute barriers that isolate the spent fuel from the surrounding environment for a long time so that the radioactivity at the time of potential canister failure has decreased significantly. In this case, if a canister is breached in the repository so that ground water can access the spent fuel, anoxic iron corrosion is expected, potentially producing a hydrogen pressure of several MPa [3]. Hydrogen has the potential to suppress the oxidative dissolution of spent nuclear fuel, as has been shown by previous works [4–8]; this hydrogen effect appears to be mainly due to the presence of noble metal inclusions (ε-particles) that allow catalysis of radiolytically formed H_2O_2 decomposition [9] and dissociation of molecular hydrogen into atomic hydrogen [10], providing a strong reductant directly at the spent fuel surface.

Since the discharge burnup of Light Water Reactor (LWR) fuel assemblies from many nuclear power plants has, in the last decades, increased from averages around 40 to 50–60 MWd/kgU, the potential effect of burnup on the dissolution process and corrosion rate of fuel has been raised as an issue for investigation. This is why some studies in the last decade or so have focused on fuels with a burnup around 60 MWd/kgU [5,6]. However, the rod burnup is varying within assemblies, the local burnup also varies axially in the rod and radially in the fuel pellet. The axial burnup typically declines rapidly near the ends of the rod giving a zone of elevated burnup in the central length region of the rod, depending on the reactor type, assembly design and the operating conditions. The radial burnup profile also includes a steep increase in the local burnup in the outermost few hundred microns of the pellet due to increased neutron moderation from the coolant and a locally elevated rate of fission.

* Corresponding author.
E-mail address: anders.puranen@svafo.se (A. Puranen).

https://doi.org/10.1016/j.jnucmat.2022.154027

The first spent fuel leaching tests aiming to determine the rate with which the spent fuel will dissolve in the repository were undertaken in the late 1970ś and were carried out in the hot cell air atmosphere. Fractional release rates for fission products such as Sr were usually used to estimate the fuel matrix dissolution rate, because uranium precipitated after a few months in a variety of U(VI) solid phases, depending on the solution composition. From the results of several such studies in a variety of groundwaters typical for different repository concepts, including salt brines, the long term Sr release rates were $\sim 3.7 \times 10^{-5}$ a^{-1} ($\sim 10^{-7} d^{-1}$) in the presence of air [11]. In these studies the effect of radiolytic oxidants, especially for γ-radiolysis was amplified by the oxygen of air, hence a few studies were carried out using inert gas flushing or anoxic conditions. The fractional release rates in presence of these much lower O_2 levels were about an order of magnitude lower [12–15].

An early systematic study of the fuel dissolution rate as a function of burnup was carried out at our laboratory [16] by leaching two-pellet segments taken from a stringer rod with varying burnup in the interval 21-49 MWd/kgU. The release rates increased with increasing burnup from 21 up to ~40-45 MWd/kgU, but afterwards decreased. In order to investigate fuel behavior at higher burnups, another study with 4 fuels segment having burnups in the interval 50 to 75 MWd/kgU (pellet burnup was calculated and also determined) was undertaken, where a fuel sample from the same rod as used in this study was also included [17]. The leaching results of these two studies, together with two other systematic studies of the fuel dissolution as function of burnup [18,19] were analyzed in [20] together with other evidence. The increase of burnup increases the concentration of fission products (such as lanthanides, Sr, Zr etc.) and actinides (Pu), making it more difficult for radiolytic oxidants to oxidize the UO_2 fuel matrix and this counteracts successfully both the increased dose rate and the subgrain formation potentially leading to a higher surface area at the pellet rim. The increased redox stability of the doped UO_2 matrix was confirmed later in studies comparing the redox reactivity of UO_2 pellets with Y or Gd-doped UO_2 or SIMFUEL [21–23]. Electrochemical studies have also shown that rare-earth doping suppresses the corrosion of UO_2 under aqueous conditions [24–27]. At the same time the concentration of the noble metal ε-particles also increases and they have a very important role in the fuel leaching under reducing conditions, catalyzing H_2O_2 decomposition [9] and activating hydrogen [10].

Since the conditions expected in the repository are reducing with excess hydrogen from Fe corrosion, it is necessary to investigate the effects of high burnup also in this environment. During the last two decades, several fuel leaching studies have been carried out in the presence of hydrogen in autoclaves in a variety of solution compositions and hydrogen partial pressures [7,11,28–34]. Fuels of burnup in the interval 40-50 MWd/kg U, including MOX fuel were tested. Such studies are much more complex than the hot cell leachings also due to the extreme ease by which U(IV) is oxidized at near neutral pH by air traces.

The outer part of the fuel pellet (rim) in fuels of burnup >40-50 MWd/kgU has a different microstructure characterised by very small grains and fission gas bubbles, referred to as High Burnup Structure (HBS) [35]. Leaching of fragments from the outer 1 mm of a 59 MWd/kgU HBU fuel pellet containing HBS under hydrogen showed similar results as the previous studies [5] and the same holds for another study with high burnup fuel (65 MWd/kgU) [6]. The results of all these studies, both with medium and high burnup, show that it seems difficult to measure oxidative dissolution rates in the presence of hydrogen [36].

The very slow dissolution rate is important in the safety assessment and small changes in the fuel may affect this, for example by changing the redox reactivity [37], microstructure [38] or other aspects that may influence interfacial processes involved in the dissolution process. Therefore, this study is performed to test the hypothesis that fuel with a burnup of 75 MWd/kgU will not dissolve faster than lower burnup fuel in repository conditions with a high hydrogen pressure.

Additionally, this experiment is in fact a close repetition but with fresh samples of fuel from the same fuel rod of a previous series of tests in the presence of hydrogen. In the previous experiments [39] we obtained difficult to interpret results, either due to the unusually high burnup of the sample (75 MWd/kgU), or more likely, to the unusually extensive pre-oxidation of the heated fuel during prolonged dry milling used for sample preparation (previous experiments performed on 250-500 µm mesh fuel powder). To avoid complications from oxidation and other effects connected to previous use of fuel samples, a fresh set of fuel fragments were taken from a nearby axial location from the same fuel rod as used by [17] and in [39]. The fuel sample was not dry milled as done for the fuel sample used in [39], rather it was simply crushed in a vice, as described in the next section.

2. Experimental

2.1. Sample description and preparation

The spent fuel (AM2K12) came from a so-called two-life rod that was irradiated in two different assemblies in both the PWRs North Anna 1 and 2, USA. As a result, a calculated rod average burnup of 70.2 MWd/kgU was reached with axial gamma scanning indicating a local pellet average burnup of 78 MWd/kgU. Fission gas release to the free rod volume was 5%. The local average linear heat generation was 18.6 kW/m (9.5 mm OD rods) with a cycle maximum of 24.3 kW/m during its first cycle. Further details on the fuel can be found in [17]. For this experiment a new section of fuel was cut out at 1000-1030 mm from the bottom end plug, a few centimeters from the axial location of the previous autoclave leaching study with this fuel. The leaching sample in [17] was taken at 945-965 mm and the isotopic analysis and local burnup assay sample from [17] was taken at 970-975 mm. The average local pellet burnup was determined at 75.4 MWd/kgU in [17] (average from Nd-contents, U-abundance and Pu-abundance measurements) a few cm below the axial position of the sample in this study.

A length of 30 mm was cut by pipe cutter from the length of rod that remained closest to the previously reported examination. A second cut was made on the 30 mm piece away from the previously exposed end giving a new piece about five millimeters high, approximately corresponding to the mid-pellet position (verified by axial gamma scanning prior to cutting). This cut was also with a pipe cutter (no cooling liquid required), and the short piece of fuel with cladding was retained. This procedure was performed to provide a distance of about 25 mm of fuel length from the previously exposed end of the fuel segment (it also gives some length of cladding to hold on to for the second cut). The short piece of fuel with cladding was then placed in an in-cell vice with a collection tray. The cladding was compressed and the resulting fuel fragments collected (Fig. 1, right). Fuel fragments amounting to 2 grams in the approximate size range of 1-2 mm mesh were collected by tweezers. Cutting and crushing was performed in a hot cell with air atmosphere. No particular tendency for the outer radial periphery of the fuel to adhere to the cladding was noted. Also the outer periphery (rim zone) was not noted to selectively undergo fine fragmentation, although the phenomenon of finer fragments from the rim (with extensive HBS, subgrain-formation) and larger fragments from the pellet center (larger grains, less residual stress) cannot be fully excluded. The local burnup of the leached samples was however assessed from the Nd, U and Pu isotopics at startup and at the conclusion of this experiment relative to the ex-

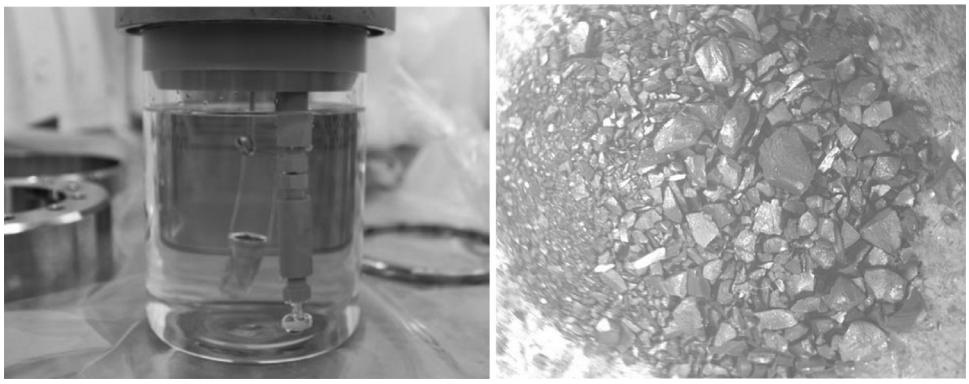

Fig. 1. Left, internal arrangement of the autoclave without the lower steel body. Right, fuel fragments after compression.

pected local burnup (see Section 3.7). The cutting and crushing operations in this experiment occurred in the latter half of November 2016, followed by pre leaching and pressurization of the autoclave with fuel on December 7th 2016. End of bombardment occurred on March 12, 2001 and the rod was punctured for gas analysis on August 7th 2002 [17].

2.2. Experimental set-up

The experiment was performed in a quartz glass beaker placed inside a stainless-steel autoclave with a twelve-bolt lid and graphite main seal supplied by PARR Inc (Fig. 1, left). The solution sampling line was fitted with a quartz filter (P4, 10-16 µm pore size) inside the autoclave. The sampling line inside the autoclave was constructed out of PEEK (PolyEtherEtherKeton) as well as the condensation drip shield covering the inside of the steel lid. This arrangement avoids any contact between the leaching solution and steel surfaces inside the autoclave.

Prior to start-up of the autoclave experiments the fuel was loaded in a fine mesh gold basket and pre-leached outside the autoclave for a cumulative time of 9 days under a slow sparging flow of Ar. The procedure involved four exposures with a brief aerated excursion when the stopper and suspended fuel basket was moved into a new flask with fresh leaching solution (200 ml each, 10 mM $NaHCO_3$). The pre-wash was performed to remove pre-oxidized surface layers from the crushing and in cell handling, as well as to remove part of the gap inventory, i.e the fraction of mobile nuclides readily accessible to water on fracture surfaces, grain boundaries, the fuel to clad interface, etc. Samples from the pre-leaching are measured to check that released U and other radionuclides are low enough, and that the release diminishes with subsequent washing exposures. The fuel was then suspended in the autoclave. The autoclave was filled with 665 ml of simplified granitic groundwater (10 mM NaCl, 2 mM $NaHCO_3$). Our solution does not contain any added Ca and Mg or Si, which are ubiquitous in groundwaters, because they would complicate the interpretation of the results since they are reported to decrease the dissolution rate of the fuel [40–42]. The autoclave was equipped with a series of valves to enable gas and solution sampling. The system was sparged with Ar + 0.003% CO_2 to eliminate residual air before being pressurized to 5 MPa of H_2.

2.3. Sampling and analytical methods

Gas samples were analyzed by gas-MS (GAM 400). The calibration protocol allowed quantification of H_2, He, N_2, O_2, Ar, Kr-80, 82, 83, 84, 85, 86, Xe-128, 129, 130, 131, 132, 134, 136. In addition a scan in the mass to charge range of 0-150 was performed for the samples to allow qualitative assessment for the potential presence of other species (such as hydrocarbons, not detected). There was no provision to sample any gases prior to pressurization of the autoclaves (no gas sampling during out of autoclave pre-leaching). Sampling of the solution was typically performed in triplicate with the first sample used for flushing of the sampling line. The second two aliquots were normally centrifuged (RCF 74kg, 1 h) and the supernatant analyzed twice per aliquot by ICP-MS (Perkin Elmer Elan DRC II or Nexion 350D), resulting in four data points for each sample. The analytical protocol was similar to that described in [17,43], although with adaptations. The analytical uncertainty depend on the isotope and concentration but generally fall in the range of ± 3-10%. No uncertainty distributions are given in the figures but the errors are typically expected to be approximately as large as the symbols used. The largest variation within duplicate samples is largely associated with very low measured concentrations or redox sensitive elements. Cs-137 was also measured radiometrically for the autoclave samples. The radionuclide inventory was calculated by the CASMO code assuming a burnup of 75.4 MWd/kgU, further details can be found in [17]. Decay correction was performed for the fractional inventory results of Sr-90 and Cs-137. Samples taken at autoclave startup and termination were also analyzed for pH and total carbonate content.

The autoclave leaching continued for 463 days during which gas was sampled 6 times and the aqueous solution was sampled 8 times at 0.125, 1, 7, 34, 91, 338, 406 and 463 days (20-30 ml per sample). No refilling or exchange of either the gas phase or the solution was performed after samplings. The experiments were performed at room temperature (~20 °C). At the last sampling of the aqueous solution a separate sample aliquot was also taken and conserved at high pH by addition to 2 M TMAH instead of nitric acid. This aliquot was utilized for a dedicated I-129 analysis by ICP-MS that was only performed for this sample.

At the end of the experiment the solution was drained from the autoclave using the solution sampling line. The basket containing the spent fuel was also removed after which the autoclave was sealed in a bag and transferred in an upright position to a fume hood. In the fume hood the autoclave lid was removed and the inner quartz glass beaker lifted out. The small amount of remaining liquid in the beaker was removed by suction. A syringe was then used to backflush the inside of the solution sampling line into the autoclave beaker and to expose all of the internal surfaces of the beaker to 2 M HNO_3. The acid was then swirled around the inside surfaces several times and left to expose the bottom of the beaker to the acid for one hour. This amount of time allows sorption/desorption equilibration in the oxidizing acid used. A sample of the rinsing acid was taken for analysis by ICP-MS to determine the precipitated or adsorbed radionuclide content on the walls and at the bottom of the vessel. The gold basket holding the spent fuel was not included in the acid rinse since complete separation of fuel fragments from the basket was considered overly hard to achieve, in addition radionuclide

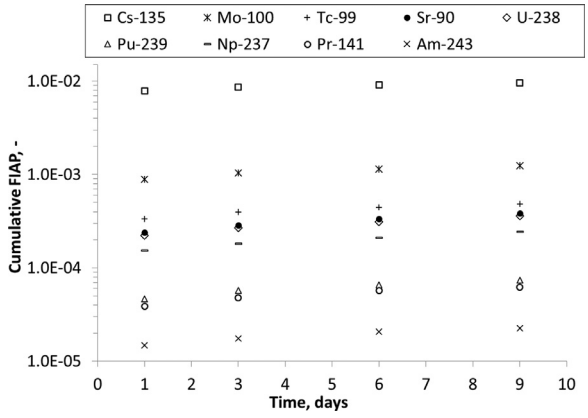

Fig. 2. Cumulative FIAP from the pre-wash of the fuel under aerated conditions.

adsorption on a gold surface was deemed to be a negligible process.

3. Results and discussion

3.1. Results of the initial aerated pre-washing of the fuel

Fig. 2 presents the results of the pre-washing of the fuel under aerated conditions. The results are expressed as the cumulative Fraction of Inventory in Aqueous Phase (FIAP). No fission gas data is collected from the pre-washing.

As can be seen in Fig. 2 the absolute majority of the pre-wash release occurs within the first day of exposing the fuel to the washing solution. In terms of concentration U-238 dominated reaching 2.9×10^{-6} M at the first exposure and 1.6×10^{-6} M or less at following exposures. The second highest release in terms of concentration was Cs-133 which reached 9×10^{-7} M at the first exposure, then declining to 1×10^{-7} M, or less at the following exposures. The inventory fractional release of Cs-135 reaches 0.80% within one day and amounted to 0.96% after 9 days in rather good agreement with Cs-137 at 1.02% and Cs-133 at 1.10% at 9 days.

3.2. Evolution of the gas phase in the autoclave

Table 1 gives the results from the autoclave gas samplings. The Kr and Xe results are the sum of the isotopes. For the first two samples after 1 and 7 days no Kr or Xe can be detected and the signal varies between no current to the low end of the typical background noise, similar to reference gases with no added Kr or Xe. At the third gas sample the Xe signal is clear, rising nearly two orders of magnitude above the noise range for the major fissiogenic isotopes Xe-136, 134, 132, while the Kr signal is weaker at only less than one order of magnitude above the noise. Ref. [17] gives the measured fission gas composition from rod puncturing. The results are in good agreement with the major Xe isotopes 136, 134, 132 and in rather good agreement with the minor Xe-131. The other Xe isotopes have very low abundances and are not useful for quantification. The three major Xe isotopes are thus used for fission gas quantification. The Kr results are not used since the results does not reproduce the expected Kr abundance due to being near or below the limit of quantification. The Xe inventory on the other hand is about an order of magnitude larger than Kr. Xe is also easier to analyze by mass spectroscopy compared to Kr (due to the higher first ionization potential of Kr). The pressures noted in Table 1 are prior to gas-sampling. The changes in gas pressure mainly come from loss of solution volume at liquid sampling occasions. The gas samples consume a very small amount of the autoclave gas since the volume of the gas sampling system is minimized and the gas sample removed in the ampoule is of a small volume at below atmospheric pressure (high vacuum pumping of sampling volume & use of fill bodies). No sampling of the solution occurred during the 245 days between gas samples G3 and G4 and the constant gas pressure (Table 1) indicates very small hydrogen consumption or leakage.

Since no replenishment of gas was performed the autoclave pressure gradually declines for each liquid sampling. The initial rapid decrease in pressure from 5 to 4.1 MPa on the first day is mainly attributed to dissolution of hydrogen into the solution which was sparged with Ar prior to pressurization of the autoclave. Similarly, the Ar gas phase concentration gradually increases due to both the initial Ar sparging of the solution off-gassing to the new gas phase and to H_2 being dissolved (and to some extent also potentially consumed). The limited increase in N_2 might indicate a small influx from the surrounding atmosphere or the seal. The O_2 level is approximately constant at a level of about 50 to 60 ppm, this could potentially be due to the system having reached an equilibrium between processes consuming O_2 and the O_2 being formed from radiolysis. The concentration of He in the autoclave rises until it reaches a plateau at about 0.6 %. This might be attributed to off-gassing of He from components in the autoclave such as the PEEK & steel components and the graphite lid seal since the autoclave was leak tested with 5 MPa of He (no solution) for several weeks just before start of the experiment. The He could also originate from the fuel since alpha decay causes a build-up of He in the fuel (the fuel rods are also pressurized with He when manufactured).

Interestingly the concentration of both Kr and Xe gradually increase during the experiment. The isotopic composition of the major Xe isotopes are in agreement with the calculated fuel inventory, proving its origin to be in autoclave Fission Gas Release (FGR). Kr isotopes were also measured, but the concentrations were very low (a few ppb). Fig. 3 show the evolution of the FGR for the major fissiogenic Xe isotopes. As can be seen the in-autoclave FGR (ie Fission Gas Released from the sample during autoclave leaching) levels off at 28±1% during the first 400 days of the experiment. This indicates that a large fraction of the fission gas, almost 30%, is decoupled from the fuel matrix, potentially being located in interconnected grain boundaries or pores that are exposed as the pres-

Table 1
Gas-MS results from the spent fuel autoclave (<DL, under Detection Limit). Initial gas pressure: 5 MPa.

Gas sample:	P1U3 G1	P1U3 G2	P1U3 G3	P1U3 G4	P1U3 G5	P1U3 G6
Kr, ppm	<DL	<DL	8.0	11.9	12.9	12.3
Xe, ppm	<DL	<DL	49.4	77.8	81.7	85.3
H_2, %	99.2	98.8	97.8	97.6	97.6	97.6
He, %	0.1	0.3	0.6	0.6	0.6	0.6
N_2, ppm	106.9	146.3	179.2	209.3	219.2	226.3
O_2, ppm	61.5	69.4	59.2	50.2	55.1	56.7
Ar, %	0.7	0.9	1.5	1.7	1.7	1.8
Pressure, MPa	4.130	3.701	3.117	3.117	2.909	2.480
Temperature,°C	21.5	21.5	21.3	21.4	20.6	20.6
Duration, days	1	7	91	336	404	459

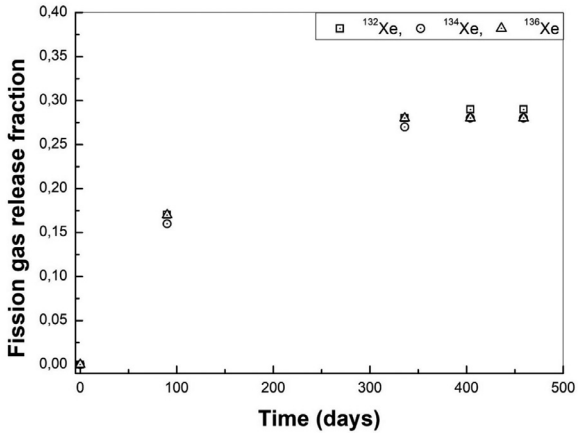

Fig. 3. Evolution of the in-autoclave fission gas fractional release of Xe-132, 134, 136.

surized water penetrates the sample. It should also be noted that the in autoclave FGR result of this study are remarkably close to the 25±2% in autoclave fission gas release for the fuel fragment leaching study in [44], in the same study the in-autoclave FGR for cladded pellets was lower although also substantial at 17±2%. Previous measurements [32] from the KIT-INE group with the same NIKUSI fuel [45] as in [44] showed about 10 times higher Xe release in Ar atmosphere than in a long-term test in presence of metallic iron, where the final H_2 partial pressure was 0.27 MPa (Table 3-4 in [32]). During fuel leaching under 4 MPa (Ar+8% H_2) the fractional releases of Kr and Xe are only slightly higher than those of Cs and lower than 1%. However, during the preceding in autoclave washing cycles under Ar of that experiment prior to hydrogen leaching a fractional release of 14.5% FGR during 292 days is reported (Table 3.3 in [32]). This suggest that the additional FGR after cutting handling and immersion mainly occurs within the first few hundreds of days. The additional FGR might also be dependent on the sampled fuel with potential parameters being initial microstructure, pressure, additives, burnup, radial temperature & power history, etc. In this context it is interesting to note that we only observed a modest in autoclave FGR of ~1-1.5% over 365 days of hydrogen exposure in [6], despite very similar procedures (also using freshly crushed fragments) and conditions to this current study.

In a study of radionuclide releases from damaged fuel rods in reactor pools, a fractional release rate for Kr-85 an order of magnitude higher than the fractional release of strontium is reported [46] (in that study Kr-85 was assayed by radiometric means which is a different methodology to the gas-MS method more suited to Xe analysis in this paper). This means that even from full length damaged fuel rods in water fission gases seem to be released from fuel faster than the matrix dissolution under oxic conditions, for which strontium is a good indicator. Finally, it should be noted that our reported releases are in addition to the in-core Xe FGR that was measured by rod puncturing at 5% [17]. The potential additional fission gas release during the years of storage after initial rod puncturing and segmentation until start of this experiment is unknown. Potential gas release during crushing and the short pre-leaching period are also unknown.

3.3. Radionuclide concentrations in the aqueous phase of the autoclave

Several studies carried out with spent fuel in the presence of hydrogen under various pressures [6,7,30,31] have demonstrated a different behavior of the uranium and other redox sensitive components of the fuel matrix after the initial part of the experiment.

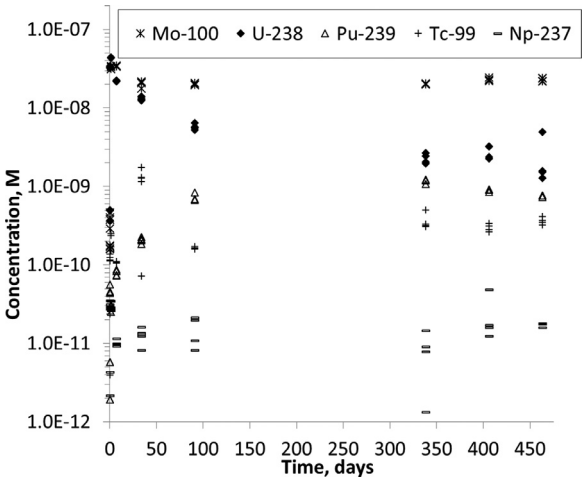

Fig. 4. Evolution of the in autoclave release of redox sensitive species Tc-99, Mo-100, Np-237, U-238 and Pu-239.

Their concentrations decrease instead of the usual increase observed in fuel leaching tests carried out in hot cell air atmosphere, due to the oxidative dissolution of the fuel matrix caused by the radiolytic oxidants produced by the strong α-, β-, and γ-radiation field of the spent fuel. This is the case also in this test, the initially attained concentrations of U, Mo, Tc decreases following the first samplings, see Fig. 4 which shows the evolution in time of the molar concentration of selected redox sensitive radionuclides in the autoclave.

The initial relatively high U and Mo concentrations in Fig. 4 can be attributed to release from pre-oxidized outer layers of the fuel matrix, as noted in several other spent fuel studies [5–7,20,21,28–31,34,39,44]. The uranium concentration (U-238) then decreases to values of ~2 to 4 $\times$ 10^{-9} M or slightly lower within one year, in good agreement with the solubility limit of UO_2 (am) [37] expected under reducing conditions. The somewhat higher measured U-238 data point of 6 $\times$ 10^{-9} M at the final sampling occasion (at 463 days duration) is associated with analysis of an additional sample that did not undergo centrifugation prior to analysis. This suggest that the uranium could in part be present in a suspended particulate form. Following an initial release the Tc-99 concentration reaches a plateau at about 5 $\times$ 10^{-10} M. The initial release of Pu-239 is very slow reaching a maximum concentration of approximately 1 $\times$ 10^{-9} M within a year, after which a slight decrease in concentration is observed. The Np-237 concentration was consistently very low throughout the experiment, in the order of 1 to 10 $\times$ 10^{-11} M. Following an initial rapid release the Mo-100 concentration was found to stabilize at 2 $\times$ 10^{-8} M. The Mo isotopic composition (based on Mo-95, 96, 97, 98, 100) was found to be in agreement with that of the calculated inventory, showing that its origin was from the fuel.

Fig. 5 shows the evolution of selected non-redox sensitive species in the autoclave.

The rapid initial release seen in Fig. 5 is probably predominantly from pre-oxidized phases and the instant release fraction. In the case of Cs and the lanthanides the release appears to cease 91 days into the experiment, suggesting depletion of the instant release fraction and inhibition of matrix dissolution. The release of Am-243 appears to cease at the following sampling at 338 days. The Sr-90 concentration appears to reach a plateau toward the end of the experiment. Together all these data from redox and non-redox sensitive radionuclides show that (1) this high burnup fuel sample does not differ significantly from lower burnup fuels with regards to radionuclide release and matrix dissolution (2) to study matrix dissolution via radionuclide release under hydrogen, exper-

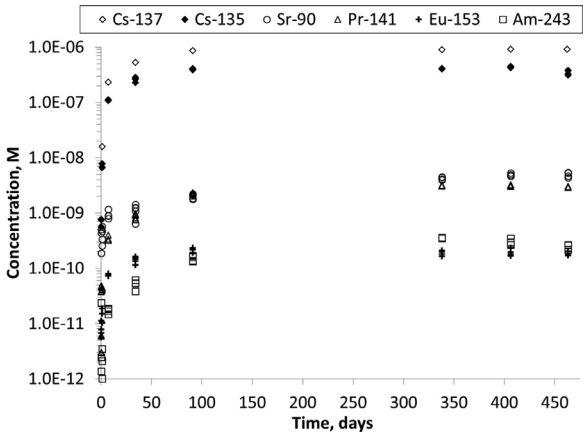

Fig. 5. Evolution of the non-redox sensitive species Sr-90, Cs-135, Cs-137, Pr-141, Eu-153 and Am-243 in the autoclave.

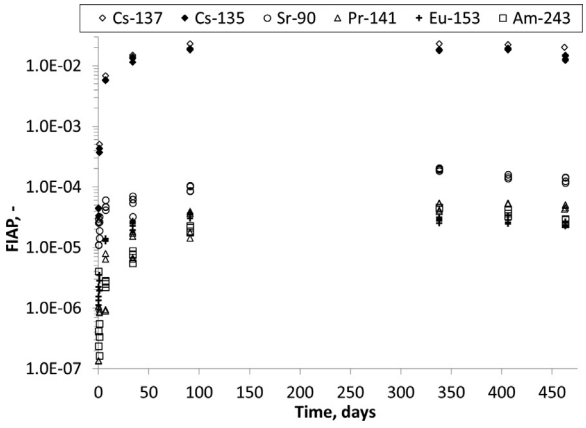

Fig. 6. Fraction of inventory in the aqueous phase for Sr-90, Cs-135, Cs-137, Pr-141, Eu-153 and Am-243 in the autoclave.

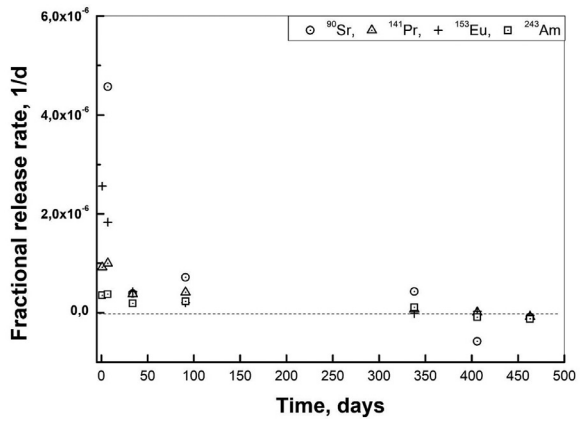

Fig. 7. Fractional release rates, 1/d for Sr-90, Pr-141, Eu-153 and Am-243 in the autoclave.

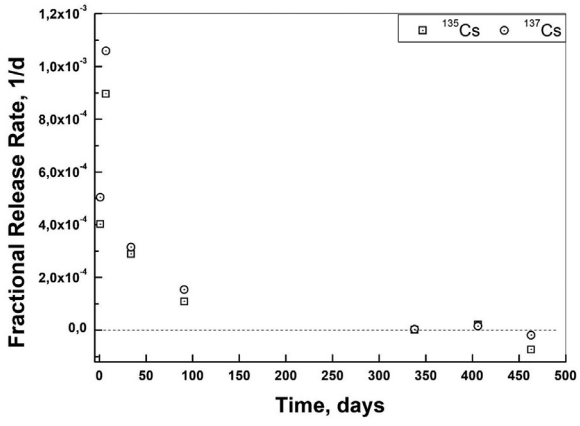

Fig. 8. Fractional release rates, 1/d for Cs-135 and Cs-137 in the autoclave.

iments need to continue for at least one year. During the first year, the results are likely still influenced by transient properties of the sample, such as remaining instant release fraction in pre-oxidized grain boundaries, high energy sites, etc. After one year, the system stabilizes.

3.4. Fractions of Inventory in the Aqueous Phase and fractional release rates

Fig. 6 presents the in autoclave Fraction of Inventory in the Aqueous Phase (FIAP) for non-redox sensitive radionuclides. It is clear that the FIAP no longer increases toward the end of the experiment. A maximum of 1.94% of the Cs-135 inventory (2.30% for Cs-137) was released to the aqueous phase during the autoclave exposure, most of that was released in the first 91 days. As was noted in Section 3.1, 0.96% of the Cs-135 inventory was also released during the pre-wash. This results in a total Cs-135 release of 2.9% for the 9 days of aerated pre-wash and the 463 days of autoclave exposure under hydrogen. This can be compared with the rod average FGR of ca 5%. The results are thus in good agreement with the previously discussed correlation of Cs/Xe release ratios of 0.6 [34,47].

An average fractional release rate ($FRR_n(X)$, units d^{-1}) during the time interval between two samplings at t_n days and t_{n-1} days may be determined from the difference between the corresponding cumulative fractional releases:

$$FRR_n(X) = [CumFIAP_n(X) - CumFIAP_{n-1}(X)]/(t_n - t_{n-1})$$
$$= FIAP_n(X) - FIAP_{n-1}(X)(1 - V_{s,n-1}/V_{tot,n-1})$$

where $V_{tot,\ n-1}$ is the total volume in autoclave before the n-1 sampling, while $V_{s,\ n-1}$ is the volume of the sample. Fig. 7 gives the fractional release rates per day for Sr-90, Pr-141, Eu-153 and Am-243.

It can be seen that Sr still has a small but positive fractional release rate up to the sampling at 338 days, after which the rate becomes negative. The rate for other radionuclides at 338 days are very near zero and scatters around a zero rate for the following samplings. Thus, these data show that there is no measureable release of these non-redox sensitive elements after one year.

Fig. 8 gives the fractional release rates per day for Cs-135 and Cs-137 which are initially over two orders of magnitudes faster than for the radionuclides in Fig. 7.

It should be noted that the Cs release rates in Fig. 8 rapidly diminish to scattering around a zero rate beyond 91 days. This initial stage of higher Cs release rate is likely related to a small amount of remaining instant release fraction in pre-oxidized grain boundaries, while when release rates scatter around zero it implies that all the remaining instant release fraction has been released, that is, the Cs that remains would be incorporated in the fuel matrix.

These results are in agreement and can be explained based on published fuel modelling studies. A common feature of most of these models is the explicit inclusion of the effect of H_2 on spent fuel dissolution rates by ε-particle catalysis. As demonstrated in the electrochemical studies in [48], ε-particles are galvanically coupled to the UO_2 matrix, i.e., they convey very negative corrosion potentials to the fuel surface in the presence of dissolved H_2. The most important process in the action of H_2 is the reduction of the oxidized U atoms on the fuel surface by electrons taken from dis-

solved H_2 via ε-particle mediation. It was shown that this process is diffusion controlled, i.e., very fast [10,49,50]. The experimental determination of kinetic constants for other important interfacial reaction rates, resulted in advanced models such as the KTH steady state model [49,51,52] and the UWO, Canada model [53,54,55].

The steady state model predicts that as little as 10 kPa H_2 (named critical H_2 concentration) will effectively inhibit the oxidative dissolution of the spent fuel aged 100 years or more, while in the presence of 1 μM Fe^{2+}, even 1 kPa H_2 will be sufficient to stop oxidative fuel dissolution [49]. Critical hydrogen concentrations that completely cancel oxidative fuel dissolution as a function of fuel age (α dose rate) are reported in [54]. For fuel with a burnup of 38 MWd/kgU and 1000 years old, the critical H_2 concentration is 3×10^{-8} M while for the alpha dose rate of a 10 000 y old fuel, the critical H_2 concentration is 5.4×10^{-9} M, corresponding to hydrogen partial pressures of 3.9 Pa respectively 0.69 Pa.

Liu et al. [55] determined the separate effects of radiolytic H_2 (internal to a fuel crack) from that produced by iron corrosion (external) on the suppression of spent fuel corrosion for different fracture or crack geometries, α-radiation dose rates and concentrations of external H_2. The hydrogen produced by α- radiolysis was found more important in suppressing fuel dissolution deep in the fractures than external H_2. Critical H_2 concentrations for suppressing dissolution of 1000 y old CANDU fuel with burnup 9.2 MWd/kgU were 5.7×10^{-6} M for fuel fractures, as compared to 3.3×10^{-7} M for planar fuel surfaces. Later, the model was successfully tested with experimental data on α-doped UO_2 dissolution and investigated also the influence of oxygen from H_2O_2 decomposition and radiolytic H_2 accumulation in a closed system on fuel dissolution [56]. The calculations showed that although the radiation dose rate, the surface coverage of ε-particles and the H_2O_2 decomposition ratio all influenced the short-term corrosion rate, the radiolytically produced H_2 had an overwhelming influence in reducing the rate below 3.3×10^{-13} mol m^{-2} a^{-1} ($<10^{-12}$ a^{-1}) after about 50 hours. It should be pointed out that in the case of this paper we deal with very high burnup fuel which also has a rather short cooling time of about 15 years and thus higher activity. We therefor utilize much higher hydrogen pressures than the predicted minimum values in the mentioned studies.

3.5. Fractions of inventory on the autoclave surfaces and estimated total releases

As was described in Section 2.3, a nitric acid rinse was performed at the end of the experiment to analyze the amount of radionuclides precipitated or adsorbed on the surfaces inside the autoclave. Table 2 gives an overview of the Fraction of Inventory in the Acid Wash (FIAW), i.e the fraction of radionuclide inventory dissolved from the autoclave surfaces by the acid wash after the autoclave was emptied of the solution used during the hydrogen exposure. Table 2 also gives the corresponding FIAP results from the pre-wash and the autoclave experiment.

The fractions recovered from the acid wash of the inner surfaces are very small in the 10^{-6} to 10^{-5} range. This corresponds to less than 20 μg of fuel found on the autoclave surfaces. Given the broadly similar fractions of inventory of the radionuclides it could be suspected that microscopic fuel fragments fell from the fuel basket onto the bottom of the autoclave and was dissolved by the acid rinse; if the data only corresponded to adsorbed or reductively precipitated nuclides, the amounts would likely be more varied depending on the distribution coefficients of the radionuclides [57,58] as we observed in [59]. The results never the less show that the autoclave beaker held minimal fractions of the inventory at the end of the experiment. There appear to be some potential discrepancies between the maximum FIAP (MAX FIAP in Table 2) values recorded during the autoclave experiment and the end values (End autoclave FIAP and FIAW in Table 2). This could potentially be attributed to re-adsorption or reductive precipitation on the fuel surface itself or on the gold basket (as noted in Section 2.3 the fuel or the gold basket was not subjected to the acid wash).

The results in Table 2 show that with the exception of Cs, for which about 2% of the inventory was released, the in autoclave release of the other radionuclides during the 463 days of duration was very modest at about 0.05 % or less. The single I-129 analysis at the end of the experiment however indicated a high release of 8.95%, this number is broadly in agreement with iodine releases being expected to be higher than those of cesium and sometimes closer to or surpassing the FGR. In that regard the I-129 release fraction of 9% is much lower than the observed in autoclave FGR of nearly 30% discussed in Section 3.2.

The overall results show that with an appropriate sample selection and preparation, avoiding extensive pre-oxidation, radionuclide releases in leaching experiments under hydrogen are low and release rates are close to zero after circa one year. Previous results using the same, high burnup fuel [39] were affected by oxidation due to dry milling and previous exposure to aerated liquids, and not representative of intact fuel behavior in the expected repository environment. In our laboratory we also milled the same (AM2K12) HBU fuel in another test down to separate fuel grains very fast (minutes), but in the presence of water solution [60]. This may be useful information for other researchers which need to mill HBU fuel.

3.6. Total carbonate and pH results

At startup the autoclave solution was measured at pH 8.2 with a total carbonate content of 123 ppm which is in line with the nominal carbonate content of 2 mM $NaHCO_3$. At the conclusion of the experiment the pH was measured at 9.2 with a carbonate content of 90 ppm.

Table 2
Fractions of Inventory released in Acid Wash, the pre-wash and during the autoclave experiment (FIAW: Fraction of Inventory in Acid Wash; FIAP: Fraction of Inventory in Aqueous Phase; NA: Not Available).

	FIAW(Autoclave acid wash)	End autoclave FIAP	Max autoclave FIAP	Pre-wash FIAP
Sr-90	2.35E-05	1.21E-04	2.04E-04	3.86E-04
Tc-99	4.19E-06	6.28E-06	3.69E-05	4.84E-04
Mo-100	5.94E-06	2.53E-04	5.53E-04	1.25E-03
I-129	NA	8.95E-02	NA	NA
Cs-135	3.06E-05	1.25E-02	1.94E-02	9.61E-03
Pr-141	1.62E-05	4.31E-05	5.40E-05	6.25E-05
Eu-153	1.13E-05	2.46E-05	3.71E-05	6.41E-05
Np-237	8.58E-06	1.15E-06	3.47E-06	2.45E-04
U-238	1.11E-05	2.05E-07	4.17E-06	3.59E-04
Pu-239	1.27E-05	7.97E-06	1.50E-05	1.23E-03
Am-243	1.50E-05	2.66E-05	4.59E-05	1.20E-03

3.7. Local burnup estimation from isotopic ratios

The pellet average local burnup was determined to be 75.4 MWd/kgU based on the chemical inventory analysis performed on a sample taken only a few centimeters below the sample that was used in this study and inventory calculations performed by the CASMO code. Section 2.1 and [17] provides further details. In order to validate the burnup assumption the U-236/235 ratio in the pre-washing samples was evaluated, the ratio scatter from 2.96 to 3.19 with an average of 3.03 resulting in a burnup of about 76 to 78 MWd/kgU for the studied sample. Section 2.5.7 in [17] provides a figure of the U-236/235 ratio vs burnup. The results from the acid wash at the conclusion of the experiment give the same results. The Pu-239 abundance at 43% however indicates a slightly lower local burnup of 74 MWd/kgU. The Nd-abundances scatter a bit but support a local burnup in the range of 75-80 MWd/kgU. The burnup of the leached sample was found to be sufficiently close to the assumed local burnup of 75.4 MWd/kgU of the inventory calculation. A conservative observation could however be added in that the local burnup could potentially be slightly higher and thus result in a slight overestimation of the released fractions of inventory.

4. Conclusions

Light water reactor fuels with burnup up to 75 MWd/kgU do not fundamentally differ from lower burnup fuel with regards to corrosion and dissolution behavior both under oxic conditions [17–20] and under reducing conditions [5–7,11,28–34].

This study demonstrates that hydrogen suppresses oxidative fuel matrix dissolution even for very high burnup fuels with a relatively short cooling time of 15 years. After one year of leaching, the system has stabilized and the uranium concentration is on the level of the solubility of U(IV). Other redox sensitive radionuclides also indicate an equilibrium with the reduced forms of their corresponding oxides.

After an initial rapid release, Cs release rates approach zero after 91 days. After one year, no further Cs release can be measured. The release rate of Sr is very low and is around zero after one year of leaching.

Combining all released fractions of Cs from sample washing, release in autoclave and acid rinse, the total fraction of Cs released is 3%. This is approximately what is expected based on the FGR of the fuel and corroborates the suggestion that the instant release fraction of Cs is less than the rod average FGR at end of irradiation.

Fission gases released during leaching in the autoclave reaches a maximum after ca 400 days. The FGR is almost 30%, significantly higher than the in autoclave I-129 release which was about 9%. The kinetics of the I release is however unknown being based on a single sample at the end of the autoclave experiment. Neither fission gases nor I was measured during the pre-washing of the fuels.

The unexpectedly high in autoclave FGR could potentially be due to hydrostatic water penetration from the autoclave pressure after prolonged storage of the fuel segment at atmospheric pressure. This could possibly be linked to transient oxidation of grain boundaries from water alpha radiolysis opening additional gas release paths. The results in [55] do however suggest that radiolysis in fractures require minimal hydrogen pressures for inhibition of the corrosion. Additional studies are required on the topic of the observed in autoclave FGR.

The overall results of this study show that it is very difficult to detect any oxidative fuel dissolution after approximately 100 days. Lower releases are observed than in our previous experiments [39] with other portions of fuel from the same rod under similar hydrogen conditions but with much more extensive fuel oxidation during prolonged dry milling prior to the transition to hydrogen conditions. The results thus support the conclusion that extensive preceding oxidation of the fuel surfaces might be detrimental for the ability of dissolved hydrogen to inhibit further corrosion of the fuel matrix. Further studies are needed to elucidate the potential long-term behavior of damaged fuel in this regard. The results never the less show that for the bulk of the spent fuel inventories, which are intact, very high burnup in itself does not seem to be a negative attribute from a deep disposal fuel corrosion and dissolution perspective.

Declaration of Competing Interest

The authors declare that they have no known competing financial interests or personal relationships that could have appeared to influence the work reported in this paper.

CRediT authorship contribution statement

A. Puranen: Writing – original draft, Writing – review & editing, Investigation. **L-Z. Evins:** Conceptualization, Writing – review & editing, Funding acquisition. **A. Barreiro:** Investigation, Validation, Writing – review & editing. **O. Roth:** Project administration, Funding acquisition. **K. Spahiu:** Conceptualization, Writing – review & editing.

Data availability

The raw/processed data required to reproduce these findings cannot be shared at this time due to technical or time limitations.

Acknowledgment

The authors would like to thank the staff at the hot cell laboratory at Studsvik Nuclear AB. AB SVAFO is acknowledged for allocating time to finalize this paper. The Swedish Nuclear Fuel and Waste Management Company, SKB, is acknowledged for financial support. Westinghouse Electric Sweden is acknowledged for the permission to use the fuel.

References

[1] SKB, Fuel and canister process report for the safety assessment SR-Can. SKB Technical Report, TR-06-22, Svensk Kärnbränslehantering AB, 2006.
[2] L. Agrenius, K. Spahiu, Criticality effects of long-term changes in material compositions and geometry in disposal canisters. SKB Technical Report, TR-16-06, Svensk Kärnbränslehantering AB, 2016.
[3] B. Bonin, M. Colin, A. Dutfoy, Pressure building during early stages of gas production in a radioactive waste repository, J. Nucl. Mater. 281 (2000) 1–14.
[4] M. Jonsson, Radiation effects on materials used in geological repositories for spent nuclear fuel, ISRN Mater. Sci. 2012 (2012) 13 Article ID 639520pages.
[5] P. Fors, P. Carbol, S. Van Winckel, K. Spahiu, Corrosion of high burn-up structured UO_2 fuel in presence of dissolved H_2, J. Nucl. Mater. 394 (2009) 1–8.
[6] A. Puranen, O. Roth, L-Z. Evins, K. Spahiu, Aqueous leaching of high burnup UO_2 fuel under hydrogen conditions, MRS Adv. 3 (19) (2018) 1013–1018, doi:10.1016/j.jnucmat.2020.152423.
[7] E. Ekeroth, M. Granfors, D. Schild, K. Spahiu, The effect of temperature and fuel surface area on spent nuclear fuel dissolution kinetics under H_2 atmosphere, J. Nucl. Mater. 531 (2020) 151981.
[8] D. Cui, E. Ekeroth, P. Fors, K. Spahiu, Surface mediated process in the interaction of spent fuel or α-doped UO_2 with H_2, MRS Symp. Proc. 1104 (2008) 87–99.
[9] D.W. Shoesmith, Fuel corrosion processes under waste disposal conditions, J. Nucl. Mater. 282 (2000) 1–31.
[10] M. Trummer, O. Roth, M. Jonsson, H_2 inhibition of radiation induced oxidative dissolution of spent fuel, J. Nucl. Mater. 383 (2009) 226–230.
[11] A. Loida, R. Gens, C. Bube, K. Lemmens, C. Cachoir, T. Mennecart, B. Kienzler, Corrosion behavior of spent fuel in high pH solutions-effect of hydrogen, MRS Symp. Proc. 1475 (2012) 119–124.
[12] R.S. Forsyth, L.O. Werme, J. Bruno, The corrosion of spent UO_2 fuel in synthetic groundwater, J. Nucl. Mater. 138 (1986) 1–15.
[13] L.H. Johnson, The dissolution of irradiated UO2 fuel in groundwater. Report AECL-6837. Atomic Energy Canada Limited, Pinawa, Manitoba, Canada, 1982.
[14] A. Loida, B. Grambow, H. Geckeis, Anoxic corrosion of various high burnup samples, J. Nucl. Mater. 238 (1996) 11–22.

[15] L.H. Johnson, D.W. Shoesmith, Spent fuel, in: W Lutze, R.C. Ewing (Eds.), Radioactive Waste Forms for the Future, North-Holland Physics Publishing, The Netherlands, 1988.

[16] R. Forsyth, The SKB Corrosion Programme. An evaluation of results from the experimental programme performed in the Studsvik Hot Cell Laboratory, SKB Technical Report, TR-97-25, Svensk Kärnbränslehantering AB, 1997.

[17] H-U Zwicky, J Low, E. Ekeroth, SKB Technical Report TR-11-03, 2011.

[18] B. Hanson, Examining the conservatisms in dissolution rates of commercial spent nuclear fuel, in: Proc. 12th Int. High-Level Waste Management Conf., Las Vegas, American Nuclear Society, 2008, pp. 404–411.

[19] C. Jegou, S. Peuget, V. Brudic, D. Roudil, X. Deschanels, J.M. Bart, Identification of the mechanism limiting the alteration of clad spent fuel segments in aerated carbonated groundwater, J. Nucl. Mater. 326 (2004) 144–155.

[20] E. Ekeroth, J. Low, H-U. Zwicky, K. Spahiu, Corrosion studies with high burn-up LWR fuel in simulated groundwater, MRS Symp, Proc 1124 (2009) Q02–Q07.

[21] M. Trummer, B. Dahlgren, M. Jonsson, The effect of Y_2O_3 on the dynamics of oxidative dissolution of UO_2, J. Nucl. Mater. 407 (2010) 195–199.

[22] R. Pehrman, M. Trummer, C.M. Lousada, M. Jonsson, On the redox reactivity of doped UO_2 pellets—influence of dopants on the H_2O_2 decomposition mechanism, J. Nucl. Mater. 430 (2012) 6–11.

[23] A. Barreiro-Fidalgo, M. Jonsson, Radiation induced dissolution of (U, Gd)O_2 pellets in aqueous solution - a comparison to standard UO_2 pellets, J. Nucl. Mater. 514 (2019) 216–223.

[24] H. He, M. Broczkowski, K. OŃeil, D. Ofori, O. Semenikhin, D.W. Shoesmith, Corrosion of nuclear fuel (UO2) inside a failed nuclear waste container. NWMO TR-2012-09, Canada, 2012.

[25] M. Razdan, D.W. Shoesmith, Influence of trivalent dopants on the structural and electrochemical properties of UO_2, J. Electrochem. Soc. 161 (2014) H105–H113.

[26] N.Z. Liu, H.M. He, J.J. Noel, D.W. Shoesmith, The electrochemical study of Dy_2O_3 doped UO_2 in slightly alkaline sodium carbonate/bicarbonate and phosphate solutions, Electrochim. Acta 235 (2017) 654–663.

[27] N.Z. Liu, J. Kim, J. Lee, Y.S. Youn, J.G. Kim, J.Y. Kim, J.J. Noel, D.W Shoesmith, Influence of Gd doping on the structure and electrochemical behavior of UO2, Electrochim. Acta 247 (2017) 496–504.

[28] K. Spahiu, L. Werme, U-B. Eklund, The influence of near field hydrogen on actinide solubilities and spent fuel leaching, Radiochim. Acta 88 (2000) 507–511.

[29] K. Spahiu, U-B. Eklund, D. Cui, M. Lundström, The influence of near field redox conditions on spent fuel leaching, MRS. Symp. Proc. 713 (2000) 633–638.

[30] K. Spahiu, D. Cui, M. Lundström, The fate of radiolytic oxidants during spent fuel leaching in the presence of dissolved near field hydrogen, Radiochim. Acta 92 (2004) 625–629.

[31] A. Loida, B. Grambow, H. Geckeis, Spent fuel corrosion behavior in salt solution in the presence of hydrogen overpressure, Proc. of ICEM'01: The 8th Internat. Conf. on Radioactive Waste Management and Environmental Remediation, Bruges, Belgium, 2011.

[32] P. Carbol, J. Cobos-Sabate, J-P. Glatz, B. Grambow, B. Kienzler, A. Loida, A. Martinez Esparza, V. Metz, J. Quiñones, C. Ronchi, V. Rondinella, K. Spahiu (eds), D.H. Wegen, T. Wiss, The effect of dissolved hydrogen on the dissolution of 233U doped UO2(s), high burn-up spent fuel and MOX fuel. SKB TR-05-09, Svensk Kärnbränslehantering AB, 2005.

[33] A. Loida, V. Metz, B. Kienzler, H. Geckeis, Radionuclide release from high burnup spent fuel during corrosion in salt brine in the presence of hydrogen overpressure, J. Nucl. Mater. 346 (2005) 24–31.

[34] P. Carbol, P. Fors, S. Van Winckel, K. Spahiu, Corrosion of irradiated MOX fuel in presence of dissolved H_2, J. Nucl. Mater. 392 (2009) 45–54.

[35] V.V. Rondinella, T. Wiss, The high burn-up structure in nuclear fuel, Mater. Today 13 (2010) 24–32.

[36] D.W. Shoesmith, The chemistry/electrochemistry of spent nuclear fuel as a waste form, in: P.C. Burns, G.E. Simon (Eds.), Uranium: Cradle to Grave, Mineralogical Society of Canada, Quebec, 2013.

[37] R. Guillamont, T. Fanghänel, J. Fuger, I. Grenthe, V. Neck, D.A. Palmer, M.H. Rand, Update on the chemical thermodynamics of U, Np, Pu, Am and Tc, OECD NEA, North Holland, Elsevier Science Publishers B. V., Amsterdam, The Netherlands, 2003.

[38] C.L. Corkhill, E. Myllykylä D.J. Bailey, S.M. Thornber, J. Qi, P. Maldonado, M.C. Stennett, A. Hamilton, N.C. Hyatt, Contribution of energetically reactive surface features to the dissolution of CeO_2 and ThO_2 analogues for spent nuclear fuel microstructures, ACS Appl. Mater. Interfaces 6 (15) (2014) 12279–12289.

[39] A. Puranen, M. Granfors, E. Ekeroth, K. Spahiu, Lessons learned from leaching of dry milled high burnup UO_2 fuel under H_2 atmosphere, MRS Adv. 1 (62) (2016) 4169–4175.

[40] J.C. Tait, J.M. Luht, Ontario Hydro Report, 1997.

[41] B.G. Santos, J.J. Noel, D.W. Shoesmith, The influence of calcium ions on the development of acidity in corrosion products deposits on SIMFUEL, UO_2, J. Nucl. Mater. 350 (2006) 320–331.

[42] B.G. Santos, J.J Noel, D.W. Shoesmith, The influence of silica on the development of acidity in corrosion products deposits on SIMFUEL(UO_2), Corr. Sci. 48 (2006) 3852–3868.

[43] S. Röllin, K. Spahiu, U.B. Eklund, Determination of dissolution rates of spent fuel in carbonate solutions under different redox conditions with a flow-through experiment, J. Nucl. Mater. 297 (2001) 231–243.

[44] E. Gonzalez-Robles, V. Metz, D.W. Wegen, M. Herm, D. Papaioannou, E. Bohnert, R. Gretter, N. Müller, R. Nasyrow, W. de Weerd, T. Wiss, B. Kienzler, Determination of fission gas release of spent nuclear fuel in puncturing test and leaching experiments under anoxic conditions, J. Nucl. Mater. 479 (2016) 67–75.

[45] H. Assman, Advantages of oxidative UO2 sintering process "NIKUSI", European Nuclear Society Meeting (ENS86), Geneva, Switzerland, June 1-6, 1986.

[46] M. Peehs, J. Fleisch, LWR spent fuel storage behaviour, J. Nucl. Mater. 137 (1986) 190–202.

[47] L. Johnson, I. Günther-Leopold, J. Kobler Waldis, H.P. Linder, J. Low, D. Cui, E. Ekeroth, K. Spahiu, L.Z. Evins, Rapid aqueous release of fission products from high burn-up LWR fuel: experimental results and correlations with fission gas release, J. Nucl. Mater. 420 (2012) 54–62.

[48] M. Broczkowski, J. Noël, D. Shoesmith, The inhibiting effects of hydrogen on the corrosion of uranium dioxide under nuclear waste disposal conditions, J. Nucl. Mater. 346 (2005) 16–23.

[49] M. Jonsson, F. Nielsen, O. Roth, E. Ekeroth, S. Nilsson, M.M. Hossain, Radiation induced spent nuclear fuel dissolution under deep repository conditions, Environ. Sci. Technol. 41 (2007) 7087–7093.

[50] M. Trummer, S. Nilsson, M. Jonsson, On the effects of fission product noble metal inclusions on the kinetics of radiation induced dissolution of spent nuclear fuel, J. Nucl. Mater. 378 (2008) 55–59, doi:10.1016/j.jnucmat.2008.04.018.

[51] O. Roth, M. Jonsson, Oxidation of UO_2(s) in aqueous solutions, Centr. Eur. J. Chem. 6 (2008) 1–14.

[52] T.E. Eriksen, M. Jonsson, H. Merino, Modelling of time resolved and long contact time dissolution studies of spent nuclear fuel in 10 mM carbonate-A comparison between two models and experimental data, J. Nucl. Mater. 375 (2008) 331–339.

[53] L. Wu, Y. Beauregard, Z. Qin, S. Rohani, D.W. Shoesmith, A model for the influence of steel corrosion products on nuclear fuel corrosion under permanent disposal conditions, Corrosion Science 61 (2012) 83–91.

[54] N. Liu, Z. Qin, J.J. Nöel, D.W. Shoesmith, Modelling the radiolytic corrosion of α-doped UO_2 and spent nuclear fuel, J. Nucl. Mater. 494 (2017) 87–94.

[55] N. Liu, L. Wu, Z. Qin, D.W. Shoesmith, Roles of radiolytic and externally generated H_2 in the corrosion of fractured spent fuel, Environ. Sci. Technol. 50 (2016) 12348–12355.

[56] M. Trummer, M. Jonsson, Resolving the H_2 effect on radiation induced dissolution of UO_2-based spent nuclear fuel, J. Nucl. Mater. 396 (2010) 163–169, doi:10.1016/j.jnucmat.2009.10.067.

[57] D. Li, D.I. Kaplan, Sorption coefficients and molecular mechanisms of Pu, U, Np, Am and Tc to Fe (hydr)oxides, J. Hazard. Mater. 243 (2012) 1–18.

[58] P. Carbol, I. Engkvist, Compilation of radionuclide sorption coefficients for performance assessment, Svensk Kärnbränslehantering AB (1997).

[59] A. Puranen, A. Barreiro, L.-Z. Evins, K. Spahiu, Spent fuel corrosion and the impact of iron corrosion – the effects of hydrogen generation and formation of iron corrosion products, J. Nucl. Mater. 541 (2020) 152423, doi:10.1016/j.jnucmat.2020.152423.

[60] O. Roth, D. Cui, C. Askeljung, A. Puranen, L.Z. Evins, K. Spahiu, Leaching of spent nuclear fuels in aerated conditions: influences of sample preparation on radionuclide release patterns, J. Nucl. Mater. 527 (2019) 151789, doi:10.1016/j.jnucmat.2019.151789.